Available online at www.sciencedirect.com

ScienceDirect

Journal of the Franklin Institute 352 (2015) 4528–4545

Journal of The Franklin Institute

www.elsevier.com/locate/jfranklin

Landmark recognition with sparse representation classification and extreme learning machine

Jiuwen Cao[a,*], Yanfei Zhao[a], Xiaoping Lai[a], Marcus Eng Hock Ong[b,c], Chun Yin[d], Zhi Xiong Koh[b], Nan Liu[b,e]

[a]*Key Lab for IOT and Information Fusion Technology of Zhejiang, Hangzhou Dianzi University, Zhejiang 310018, China*
[b]*Department of Emergency Medicine, Singapore General Hospital, Singapore 169608, Singapore*
[c]*Health Services and Systems Research, Duke-NUS Graduate Medical School, Singapore 169857, Singapore*
[d]*School of Automation Engineering, University of Electronic Science and Technology of China, Chengdu 611731, China*
[e]*Centre for Quantitative Medicine, Duke-NUS Graduate Medical School, Singapore 169857, Singapore*

Received 6 March 2015; received in revised form 12 June 2015; accepted 2 July 2015
Available online 15 July 2015

Abstract

Along with the rapid development of intelligent mobile terminals, applications on landmark recognition attract increasingly attentions by world wide researchers in the past several years. Although promising achievements have been presented, designing a robust recognition system with an accurate recognition rate and fast response speed is still challenging. To address these issues, we propose a novel landmark recognition algorithm in this paper using the spatial pyramid kernel based bag-of-words (SPK-BoW) histogram approach with the feedforward artificial neural networks (FNN) and the sparse representation classifier (SRC). In the proposed algorithm, the SPK-BoW approach is first employed to extract features and construct an overcomplete dictionary for landmark image representation. Then, the FNN trained with the extreme learning machine (ELM) algorithm combined with the SRC is implemented for landmark image recognition. We conduct experiments using the Nanyang Technological University (NTU) campus landmark database to show that the proposed method achieves a high recognition rate than ELM and a lower response time than the sparse representation technique.

*Corresponding author.
E-mail addresses: jwcao@hdu.edu.cn (J. Cao), laixp@hdu.edu.cn (X. Lai), chunyin@uestc.edu.cn (C. Yin), liu.nan@sgh.com.sg (N. Liu).

http://dx.doi.org/10.1016/j.jfranklin.2015.07.002
0016-0032/

1. Introduction

Landmark recognition has become a popular topic in the past several years due to its wide applications in intelligent mobile equipments [1–15]. Along with the rapid development of high speed broadband network and intelligent mobile terminals, landmark recognition has been found potential applications in urban environment navigation and localization, city tourist and shopping guide, street view, etc. A general landmark recognition system can be realized in three steps, i.e., image capturing in the user's end, feature extraction and classification in the server side, and retrieved information returning to and displaying on mobile terminals. For detailed developments on landmark recognition, we refer the readers to the fruitful surveys [1,2]. Due to the limited bandwidth of mobile networks and the fast response time requirement by users, designing a robust recognition system with an accurate recognition accuracy and fast response time still remains a challenging task.

Image representation is one of the key parts in a landmark recognition system. Considerable attentions have been paid to feature extraction of landmark image in the past decade [3–8,16–28]. Achievements on landmark image representation can be broadly described in two aspects, namely, global feature [25–28] and local feature [3–8,16,17,19–24]. Exploiting the entire image characteristics, such as the pixel color, the edge information, the energy spectrum, global features usually enjoy the properties of low computational complexity and ease of implementation. However, global information has limited capability in handling landmark image containing background clutter and occlusions. Local feature extraction approaches, which investigate interest points and local cells in the image, are more robust to landmark occlusions and viewpoint changes in real applications. The scale invariant feature transform (SIFT) [32] and the affine invariant feature [33] are representative local feature extraction approaches used for landmark recognition. After collecting visual words constructed through clustering all local features, the bag-of-words (BoW) histogram is the commonly used approach for landmark image representation. To enhance the recognition performance, many BoW based representation methods have been presented. Such achievements include estimating the likelihood of local patches via a probability density response map [29], utilizing the low-level contextual information for patch saliency estimation [30], evaluating patch importance through a nonparametric density estimator [31], emphasizing the cell of interests via the spatial pyramid kernel based BoW (SPK-BoW) feature extraction [7,12], the scalable vocabulary tree (SVT) method [35], etc.

Intelligent classifier plays another key role for landmark image recognition system. An intelligent classifier with an accurate recognition rate and fast processing speed is highly desired for landmark recognition applications, especially for implementations on mobile devices. Machine learning based discriminative landmark classification approaches have been comprehensively studied in literature, including the k nearest neighborhood (k-NN) [23], the Adaboost algorithm [3], support vector machine (SVM) and its variants [6,7,26,34], artificial neural networks [12], etc. k-NN is the simplest one to be implemented for landmark recognition while its speed is relatively slow. The Adaboost algorithm has been used for web based landmark/scene image classification. SVM and its variants are popular algorithms for landmark applications due to their powerful capabilities in handling multi-class data classification. However, when dealing with high dimensional features and large scale databases, SVM suffers a high computational burden in classifier learning and a relatively long recognition time for query image. As evidenced by experiments in [7], the fuzzy SVM with the Laplacian radial basis function (RBF) kernel cost more than one thousand seconds to learn the Nanyang Technological University (NTU) campus landmark database and the recognition time for a query image is more

than several seconds. Such a long processing time makes the SVM based classifier unsuitable for landmark recognition applications in mobile terminals. To enhance the robustness of landmark classifier in handling sequential data, a fast online learning framework based on single hidden layer feedforward neural networks has been presented for landmark recognition [12]. Utilizing the recent popular extreme learning machine (ELM) algorithm [36–42], the recursive least square approach, and the SPK-BoW, the proposed algorithm has shown efficiency in updating classifier with new collected landmark samples in [12]. Other than discriminative based classifiers, the generative based approaches, which attempt to estimate the density distribution of the data, have been investigated for landmark recognition. Representative generative based techniques in landmark classification include the Bayesian classifier [10], the probabilistic latent semantic analysis approach [23], etc.

Motivated by the sparsity of the response in human visual cortex neuron [45,46], the sparse representation algorithm has been recently developed for image processing [43,44] and system identification [47]. It was shown that the sparse representation classification (SRC) is more robust and accurate in recognizing noisy images than conventional machine learning based approaches [43,44,54]. In [43], the SRC algorithm has been implemented to exploit the relationship of face images from the same category. The recognition is then formulated as solving a sparse signal representation problem through a linear regression model [43]. Rather than feature extraction, it is emphasized in [43] that correct computing of the sparse coefficients and a sufficiently large number of features are critical in face recognition. Benefiting from recent achievements in estimating the sparse signal from an underdetermined linear system in compressed sensing (CS) [48–51], the SRC algorithm shows promising performance in handling errors raised by occlusion and corruption in face images. Motivated by this novel classification framework, we have applied the SRC algorithm for landmark recognition in [53]. Two popular estimators, the orthogonal matching pursuit (OMP) [52] and the sparse reconstruction by separable approximate (SpaRSA) [44], are tested on the NTU campus landmark database. It is shown that the SRC scheme not only achieves a higher recognition rate than state-of-art algorithms but also enjoys the training-free property for classifier learning.

Although the SRC algorithm provides superiorities on landmark classification, the long recognition time issue costed by solving the optimization problem in sparse signal recovery is also spotted [53]. Experiments conducted using the NTU campus database on an ordinary PC show that the recognition time for single query landmark image spent by OMP and SpaRSA is more than several and twenty seconds, respectively. To address this issue, we propose a novel landmark recognition framework in this paper based on the efficient SPK-BoW image representation approach, the recent ELM combining with the SRC approach [54]. In the first stage, the SPK-BoW approach which exploits the spatial layout information of landmark images is used for feature extraction and visual words dictionary construction. In the second stage, to speed up the recognition procedure, the fast ELM algorithm is employed to train the FNN for query landmark images partition and classification. The output of ELM classifier for each query landmark image is used as an assessment to decide whether it should be fed to the SRC algorithm or not. In the last stage, the SRC algorithm is used to classify the query landmark images which do not have discriminative identification entry in the output vector obtained by ELM. Due to the incorporation of the ELM algorithm, the proposed landmark recognition framework is able to achieve a faster testing speed with small loss of accuracy than using the SRC algorithm alone. To show the efficiency of the proposed algorithm, we test the recognition scheme with experiments using several representative sparse recovery algorithms in CS and the performance is also compared with the SVT based image representation approach.

2. Overview on the proposed landmark recognition framework

The overview of our proposed landmark recognition framework is given in this section. To speed up the training and testing phase and to improve the recognition performance, three main steps are included in our landmark recognition algorithm. Brief introductions are given in the following.

In the first stage, the SPK-BoW approach is used for feature extraction [12]. Two level partition scheme which exploits the general trait in landmark images that the target is normally located in the central cell is adopted for landmark image representation. This fine partition is shown to be efficient in emphasizing the local patches containing the landmark information.

In the second stage, the feedforward artificial neural network is implemented as the classifier. The recent ELM is utilized as the learning algorithm for landmark data training. Comparing with conventional tuning based parameter updating approaches and the famous SVM, ELM has the advantages of extremely fast training speed and convincing generalization performance [36].

The sparse representation classification (SRC) algorithm is performed in the third stage to increase the landmark recognition rate. As illustrated in [53], SRC algorithm shows good capability in handling noise and achieves a high recognition rate in general. However, it also suffers a long recovering time issue in landmark recognition [53]. In order to reduce the average recognition time, we divide the query landmark images into two groups according to the output obtained by the ELM classifier. Only those query landmark images which do not have discriminative identification entry in the output vector obtained by ELM are fed to the SRC algorithms for classification in this stage.

To give a visualized illustration, we plot a flowchart of the proposed hybrid landmark recognition algorithm in Fig. 1. The testing landmark image will be fed to a pre-trained ELM classifier after the SPK-BoW feature extraction. The output entries in the vector obtained by the ELM classifier are then used as an assessment to decide whether the landmark image should be processed by the SRC algorithm or the classification should be maintained to use the estimation by the ELM approach.

3. Landmark recognition with SRC and ELM

In this section, the detailed descriptions of the landmark recognition using the SPK-BoW image representation approach and the hybrid classifier ELM-SRC are given. The long recognition time issue in SRC algorithms is also presented for discussions.

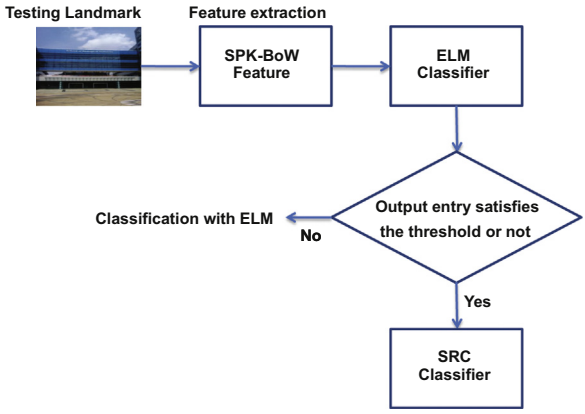

Fig. 1. The flowchart of the proposed hybrid landmark recognition algorithm.

3.1. SPK-BoW

Local feature extraction enjoys the advantage of characterizing interesting points in local cells. SIFT selects keypoints that are invariant to image scale and rotation using the difference of Gaussian (DoG) scale space as

$$\begin{aligned}\mathbf{D}(x,y,k\sigma) &= [G(x,y,k\sigma) - G(x,y,\sigma)] \otimes \mathbf{I}(x,y) \\ &= \mathbf{L}(x,y,k\sigma) - \mathbf{L}(x,y,\sigma) \end{aligned} \tag{1}$$

Here, $G(x,y,\sigma)$ is the Gaussian function, k denotes the scale, and $\mathbf{I}(x,y)$ is the image with x and y representing the space coordinates, and $\mathbf{D}(x,y,k\sigma)$ is the resulting DoG scale convolved with the image. Then, descriptors are extracted by computing orientation histograms in the local regions around the keypoints. The descriptors are robust to changes in illumination, viewpoint, occlusion and background clutters. An example of using SIFT descriptors for matching two images is illustrated in Fig. 2. The two images are taken on the same landmark but from different viewpoints. The lines connecting the two images indicate the SIFT points that are matched between the two images. SIFT feature is a local feature. Compared with traditional overall feature, it improves the efficiency of the method.

Direct adopting the SIFT feature for classifier training may not be suitable for mobile landmark recognition due to the high computational cost used by the large number of dense feature vectors, e.g., for an image of 240×320 pixels, the number of dense SIFT vectors extracted from 8×8 (pixels) patches will be 1200. This large number increases the computation cost greatly and lowers down the computation speed. To reduce the number of features, the bag-of-words (BoW), which are originally developed for text representation and retrieval, are used in this paper [22]. BoW has been proven to obtain a quite good recognition performance compared with keypoint-based and multi-scale-based representations in several landmark recognition works [23,24]. It quantizes the dense SIFT vectors into a several hundred-dimensional histogram according to the previously constructed codebook. The recognition time will be greatly reduced, and users' real-time information retrieval requirements can also be satisfied.

However, when employed for landmark recognition systems, conventional BoW algorithms usually ignore the spatial layout information of landmark images. That is, in landmark images, the area of interests usually locate in the central while background image normally distributes in the borders, such as sky, land, grass, etc. To exploit the spatial layout information, a level

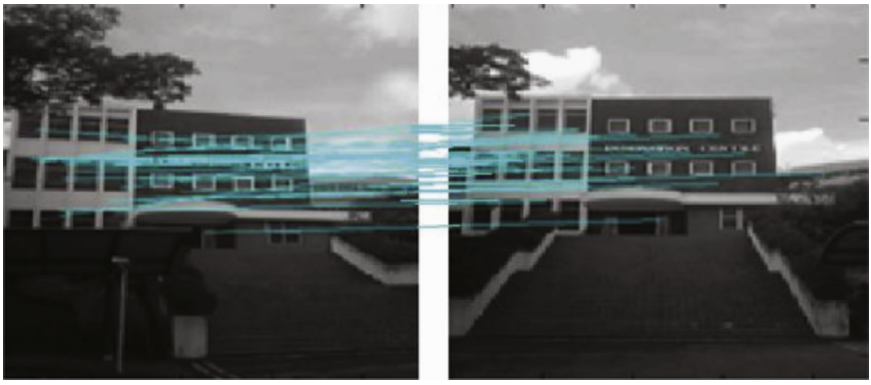

Fig. 2. Illustration of matching SIFT keypoints extracted from two images (the Innovation center in NTU campus).

partition scheme which divides the image into 1×1, 2×2, and 4×4 levels has been presented in [18]. However, the 2×2 strategy is not reasonable for landmark image as the partition tends to mix up foreground and background areas [12], which leads to meaningless local cells. To address this issue and emphasize the area of interest, we adopt the spatial pyramid decomposition scheme which separates the landmark images into 1×1 and $(1 \times 3) + (3 \times 1)$ two levels in our paper [12]. As illustrated in Fig. 3, the partition method in level 2 has a high chance to separate the image into landmark areas and background areas. After the decomposition, the local features are calculated in each cell at each pyramid level and the histograms computed from each local patch are then concatenated into a high dimensional vector for image representation.

3.2. SRC

3.2.1. The SRC algorithm

The sparse representation classification (SRC) algorithm is motivated by the sparsity of the response in human visual cortex neuron [45,46]. The SRC algorithm is to decompose the query signal throughout an overcomplete dictionary, where each column of the dictionary is called a basis atom and is extracted from known objects or signals. The sparse coefficients are calculated by mapping the query signal to the characteristic sub-space formed by those atoms in the dictionary with the same category of the query signal. The classification is then performed by computing the minimum reconstruction error. Benefiting from recent achievements in compressed sensing (CS), a lot of sparse signal sampling and reconstruction techniques can be employed in the SRC algorithm [44,48–52].

In CS, the problem of sparse signal reconstruction is expressed as in an underdetermined linear system $\boldsymbol{y} = \Phi \boldsymbol{x}$, where $\Phi \in R^{m \times n}$ and $m \ll n, \boldsymbol{x}$ is solvable given that the measurement matrix Φ satisfies the *restricted isometry property* (RIP) and $\boldsymbol{x}$ is sparse [48,49]. The ℓ_1 norm minimization problem is formulated for sparse signal recovery in the following:

$$\min_{\boldsymbol{x} \in R^n} \|\boldsymbol{x}\|_{\ell_1} \quad \text{s.t. } \boldsymbol{y} = \Phi \boldsymbol{x} \tag{2}$$

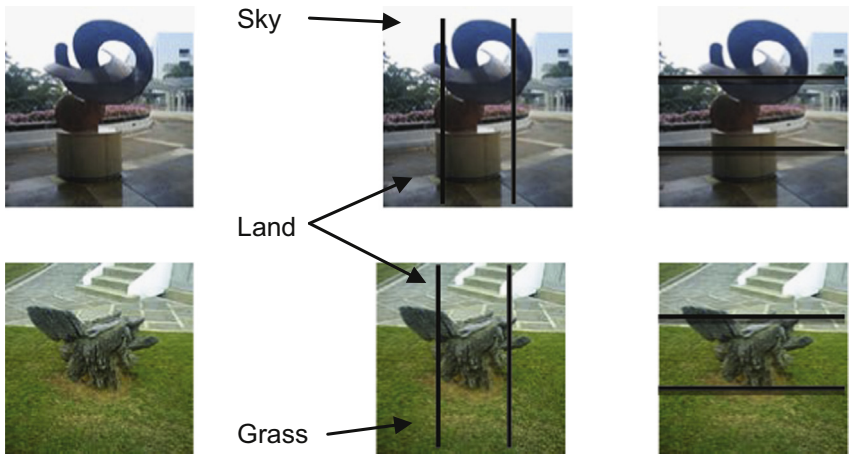

Fig. 3. The two level spatial pyramid sampling strategy on landmark images from NTU campus database.

where $\|\boldsymbol{x}\|_{\ell_1} = \sum_{i=1}^{n} |x_i|$ and x_i is the i-th entry in $\boldsymbol{x}$. The RIP definition of the sampling matrix $\boldsymbol{\Phi}$ is

Definition 1. The sampling matrix $\boldsymbol{\Phi}$ is said to hold the RIP with parameter $\epsilon \in (0,1)$ if the following inequality satisfies

$$(1-\epsilon)\|\boldsymbol{x}\|_2^2 \le \|\boldsymbol{\Phi x}\|_2^2 \le (1+\epsilon)\|\boldsymbol{x}\|_2^2$$

where ϵ is called the *restricted isometry constant* (RIC), $\boldsymbol{x}$ is sparse with $\boldsymbol{x} \in \{\boldsymbol{x} \in R^n | \|\boldsymbol{x}\|_0 \le k, k \ll n\}$ and $\|\boldsymbol{x}\|_0$ denotes the support of the signal $\boldsymbol{x}$.

The SRC algorithm is originally developed for face recognition [43,54] and then extended to landmark image classification [53]. Exploiting the relationship between the query sample and the training data from the same category, the classification is performed by solving a linear representation problem. In general, the coefficient is sparse given that sufficiently large number of training samples are collected for each category in the dictionary.

Combined with the above SPK-BoW image representation, the SRC algorithm has been implemented for landmark classification in [53] for the first time. Constructing the matrix $A_k = [\boldsymbol{w}_{k,1}, \boldsymbol{w}_{k,2}, \ldots, \boldsymbol{w}_{k,n_k}] \in R^{m \times n_k}$ using SPK-BoW histograms of training samples belonging to the k-th landmark category, the query landmark image $\boldsymbol{y}$ from the same category can be represented using the atoms in the matrix A_k as

$$\boldsymbol{y} = \alpha_{k,1}\boldsymbol{w}_{k,1} + \alpha_{k,2}\boldsymbol{w}_{k,2} + \cdots + \alpha_{k,n_k}\boldsymbol{w}_{k,n_k}. \tag{3}$$

Here, m and n_k denote the dimension of the extracted landmark feature vectors and the number of training samples in the k-th category, respectively, and $\alpha_{k,1} \in R$, $k = 1, 2, \ldots, n_k$. With samples from all landmark categories and sufficient number of training data, the linear representation can be written in the following expression:

$$\boldsymbol{y} = A\boldsymbol{x} \tag{4}$$

where $A = [A_1, A_2, \ldots, A_K] \in R^{m \times n}$ the dictionary built by concatenating feature vectors of all training samples as the column vectors, $n = \sum_{k=1}^{K} n_k (k = 1, \ldots, K)$, K is the number of categories and $\boldsymbol{x} = [\boldsymbol{0}, \ldots, \boldsymbol{0}_{k-1}, \alpha_{k,1}, \ldots, \alpha_{k,n_k}, \boldsymbol{0}_{k+1}, \ldots, \boldsymbol{0}_K]^T$. Here, $\boldsymbol{0}$ denotes the zero vector. The ideal solution $\boldsymbol{x}$ is a sparse vector. Then, the classification is to estimate the sparse solution from the underdetermined linear system and find the associated categories of the atoms where these sparse coefficients are related to. To illustrate this, we plot the estimated sparse coefficients for a query landmark using the SpaRSA algorithm [44] with experiments on the NTU campus database in Fig. 4(a). In this framework, 3532 landmarks from 50 different categories are used to construct the dictionary matrix A in Eq. (4). The coefficients of the associated training landmarks with the same category to the query image are labeled with red circle "**o**" in Fig. 4(a). One can spot from the curve that coefficients of the training samples with the same label to the testing landmark play dominant roles in the linear representation.

In order to successfully explore the sparse coefficients derived by Eq. (4), the recognition of a query landmark image is transferred to calculate the residual by evaluating how well the coefficients associated with all training samples of each object reproduce $\boldsymbol{y}$ [43,53]. Defining the characteristic function $\psi_k(\tilde{\boldsymbol{x}})$ which only selects the coefficients in $\tilde{\boldsymbol{x}}$ associated to the k-th landmark, classifying the query landmark image $\boldsymbol{y}$ becomes finding the minimal residual problem

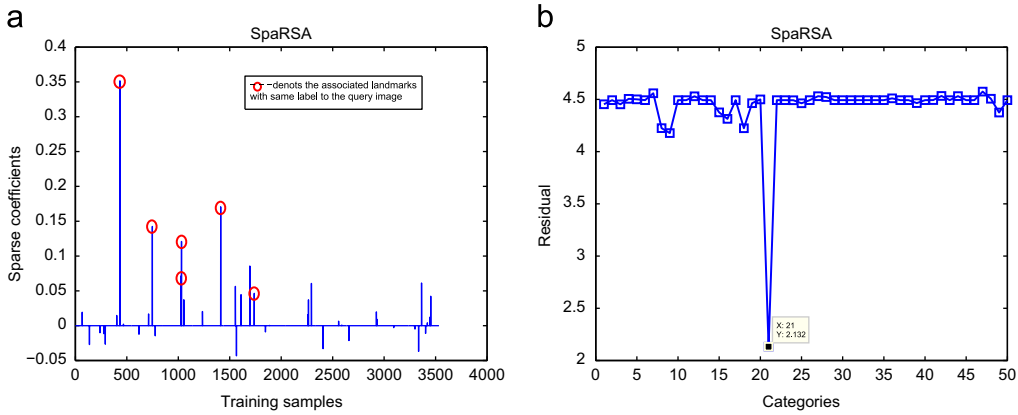

Fig. 4. The sparse coefficients of the linear representation and residuals for a query landmark image with the SpaRSA algorithm. (For interpretation of the references to color in this figure, the reader is referred to the web version of this paper.)

expressed as follows [53]:

$$c_y = \underset{k}{\operatorname{argmin}}\{r(\tilde{\boldsymbol{y}}_k)\}, \quad k = 1, \ldots, K$$
$$\text{with} \quad r(\tilde{\boldsymbol{y}}_k) = \|\boldsymbol{y} - \tilde{\boldsymbol{y}}_k\|_2,$$
$$\tilde{\boldsymbol{y}}_k = A\psi_k(\tilde{\boldsymbol{x}}). \tag{5}$$

Here, $\tilde{\boldsymbol{x}}$ is the estimated sparse signal in Eq. (4). A detailed description of the SRC algorithm for landmark recognition using the SPK-BoW feature is given in Algorithm 1.

Algorithm 1. The SRC algorithm for landmark recognition.

Given:

The SPK-BoW feature dictionary of training landmarks A;

The number of landmark categories K

Output:

(1) For each testing landmark, extract its SPK-BoW histogram $\boldsymbol{y}$

(2) Estimate the sparse coefficient $\tilde{\boldsymbol{x}}$ through ℓ_1-minimization problem

$$\tilde{\boldsymbol{x}} = \underset{\boldsymbol{x}}{\operatorname{argmin}} \|\boldsymbol{x}\|_1 \quad \text{s.t.} \quad A\boldsymbol{x} = \boldsymbol{y}$$

(3)● **for** $k = 1 : K$

- Find the vector $\varphi_k(\tilde{\boldsymbol{x}})$
- Calculate the residual $r(\tilde{\boldsymbol{y}}_k) = \|\boldsymbol{y} - \tilde{\boldsymbol{y}}_k\|_2$, with $\tilde{\boldsymbol{y}}_k = A\psi_k(\tilde{\boldsymbol{x}})$
- **end for**

(4) The category of the query landmark is

$$c_y = \arg \min_{k \in [1,\ldots,K]} \{r(\tilde{\boldsymbol{y}}_k)\}$$

An experimental result using the NTU campus landmark database is also presented in Fig. 4(b) to verify the residual based classification in SRC. As shown in the figure, the residual of the reproduced feature using the coefficients in $\tilde{\boldsymbol{x}}$ associated to the correct category (the 21-th category) is apparently lower than the rest residuals. Experimental comparisons to the popular

SVM and the ELM based feedforward neural network in [53] demonstrated that the SRC algorithm is able to achieve higher recognition rate.

3.2.2. Long recovery time issue in SRC

Compared with conventional machine learning based approaches, although the SRC algorithm does not need the classifier training procedure, the long recognition time issue is also spotted in [53,54]. The computational cost is incurred by the ℓ_1 norm minimization in sparse signal estimation. In general, the more the training samples and the larger the feature dimensional are, the higher the computational complexity in SRC is.

Figure 5 plots the recognition time per sample spent by the SRC algorithm on the NTU campus database for demonstration. Two representative sparse signal recovery algorithms, namely the orthogonal matching pursuit [52] and the SpaRSA algorithm [44], are compared and two different numbers of feature vectors 200 and 1400 are tested for illustration. As observed from the curve, the recognition time for single query sample by the SpaRSA approach is more than 2 s when using 200 features while for 1400 features, it is longer than 24 s. For the OMP algorithm, the recognition time seems acceptable. However, as reported in [53], the recognition performance is worse than the one by the SpaRSA approach. The long recovery time limits the implementation of SRC algorithm for landmark recognition in mobile terminals.

3.3. Landmark recognition with ELM-SRC

To address the long recognition issue in SRC, we employ the hybrid method by combining the recent ELM based feedforward neural network and the SRC algorithm (ELM-SRC) [36,38,54] for landmark recognition in this paper. Benefiting from the randomness property and the network parameter tuning-free strategy, the ELM algorithm is incorporated into the recognition scheme to speed up the process. In the first stage, the ELM algorithm is implemented for feedforward neural network training and landmark classification. In the second stage, the query images which contain high noise are processed via the SRC algorithm. For query landmarks, the output of the ELM classifier is used as a judgement to decide which samples should be identified through the SRC algorithm. The detailed

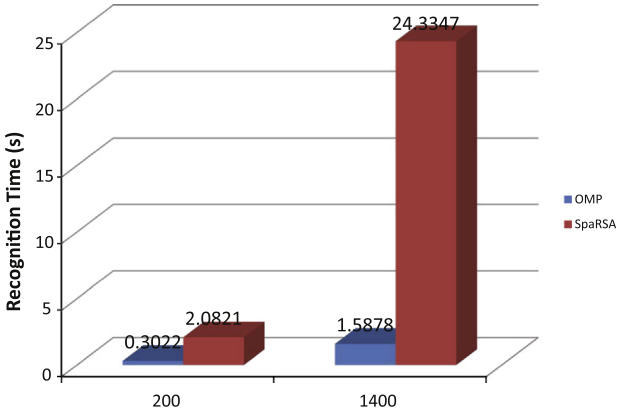

Fig. 5. Recognition time per sample comparisons of SRC algorithms with OMP and SpaRSA.

description of the basic ELM classifier and the ELM-SRC landmark recognition framework are given in the following.

3.3.1. Basic ELM algorithm

Given a training data $\mathcal{A}=\{(\mathbf{x}_i,\mathbf{t}_i)\}_{i=1}^{\mathbf{N}}$, the output function of the single hidden layer feedforward neural network (SLFN) with L hidden neurons can be expressed as

$$f(\mathbf{x}_i)=\sum_{j=1}^{L}\boldsymbol{\beta}_j h_j(\boldsymbol{a}_j,b_j,\mathbf{x}_i)=\mathbf{h}(\mathbf{x}_i)\boldsymbol{\beta},\quad i=1,\ldots,\mathbf{N} \tag{6}$$

where $\boldsymbol{\beta}=[\boldsymbol{\beta}_1,\ldots,\boldsymbol{\beta}_L]^T$ is the output weight matrix, $\mathbf{h}(\mathbf{x}_i)=[h_1(\boldsymbol{a}_1,b_1,\mathbf{x}_i),\ldots,h_j(\boldsymbol{a}_L,b_L,\mathbf{x}_i)]$ is the network output corresponding to the training sample $\mathbf{x}_i$, $h_j(\cdot)$ is a nonlinear piecewise continuous function, and $\boldsymbol{a}_j\in\mathcal{R}^d$ and $b_j\in\mathcal{R}$ $(j=1,2,\ldots,L)$ are parameters of the jth hidden node, respectively. The purpose of network training is to find suitable network parameters to minimize the error function $\|\mathbf{H}\boldsymbol{\beta}-\mathbf{T}\|_2$, where

$$\mathbf{H}=\begin{bmatrix}\mathbf{h}(\mathbf{x}_1)\\ \vdots\\ \mathbf{h}(\mathbf{x}_\mathbf{N})\end{bmatrix}\quad\text{and}\quad\mathbf{T}=\begin{bmatrix}\mathbf{t}_1^T\\ \vdots\\ \mathbf{t}_\mathbf{N}^T\end{bmatrix} \tag{7}$$

are the hidden layer output matrix and the target output, respectively. ELM theories argue that for any nonlinear piecewise continuous activation function, the hidden node parameters can be generated independent of training data according to any continuous sampling distribution probability. Such parameters need not be tuned during the learning stage. The neural network training then becomes analytically tractable by solving an inverse problem of a linear system. The universal approximation capability has been provided in [55] to support the ELM algorithm. These properties enable the ELM algorithm an extremely fast learning speed and reliable generalization performance.

For multi-class classification problem, ELM generally transfers to it a high dimensional regression problem. The One-Against-All (OAA) method is the mostly used strategy in ELM [40]. For a K category application, the output label for the i-th sample is mapped to a K-dimensional vector $\mathbf{t}_i=(t_{i1},t_{i2},\ldots,t_{iK})^T$, where the entry in $\mathbf{t}_i$ whose index is identical to the sample is set to be 1 while the rest entries are set to be -1. For example, if the label for the i-th sample is k, then, with the OAA approach, the K-dimensional vector is

$$\mathbf{t}_i=\left(-1,\ldots,-1,\underset{\substack{\downarrow\\ t_{ik}}}{1},-1,\ \ldots,\ -1\right)^T. \tag{8}$$

The classification of testing samples in ELM is performed by finding the index of the largest entry in the network output.

3.3.2. The ELM-SRC algorithm for landmark recognition

To speed up the recognition process, ELM is involved in classifying the landmark image in the SRC algorithm. The reason for choosing ELM rather than SVM is that ELM provides fast data processing speed and good generalization performance [56]. After building the classifier with training landmarks, ELM is adopted to identify query landmarks with discriminative features while for those query landmarks containing high level noise, the SRC algorithm is performed for recognition.

To decide which query image should be processed by the SRC approach while which one should be left to the ELM classifier, the estimated output vector of the query landmark by the ELM classifier is utilized as a judgement as suggested in [54]. Since the OAA decomposition approach is implemented to transfer the classification problem to a multi-output regression problem and the category identification of the testing sample in the feedforward neural network relies on searching the index of the largest entry in the output vector, it is believed that for query sample with discriminative features and less noise, its entry with the index associated to the correct category should be larger than the rest entries in general. In other words, the entry with the index associated to the correct category may not be markedly larger than the rest entries or the query sample may be mislabeled if it contains high level noise. In view of this, we use the estimated output vector of the ELM classifier as an assessment and employ the SRC algorithm to handle those query landmarks with less discriminative features and high noise. Thus, as stated in [54], the difference between the peak value o_p and the second largest value o_s in the outputs is used as the criteria. That is, for a query landmark, the output of the ELM classifier is

$$\mathbf{o} = (o_1, \ldots, o_K)^T \in R^K. \tag{9}$$

The sample is treated using the ELM classifier if the following inequality holds:

$$o_p - o_s > \delta \tag{10}$$

where δ is a small positive scalar. Otherwise, the query image is considered containing high level noise and is then classified through the SRC algorithm. It is apparent that a proper choice of δ is critical. A few samples will be selected for the SRC algorithm if a small value is assigned to δ, vice versa. In general, a large value is able to assign a few number of testing samples to ELM, where these testing landmark images contain less noise and are easy to be correctly classified. However, it also means more samples will be handled by the SRC algorithm. Although the classification accuracy derived by the hybrid classifier ELM-SRC maintains as good as SRC, but it also suffers a long testing time per sample. On the contrary, a large number of testing samples can be chose for ELM classifier if a small difference value is used as the threshold. Although, it can help to reduce the average testing time, the recognition also decreases as only fewer samples have been assigned to the SRC algorithm. Experimental results in [54] suggest that most of the misclassified samples can be picked out when δ is around 0.5.

After dividing the query landmark database into two sub-groups, those samples with low difference value $(o_p - o_s)$ are fed to the SRC algorithm for classification. The recovery algorithm is the key part in the SRC approach. For implementation in landmark recognition, fast sparse signal reconstruction speed and accurate estimation performance are two essential points. In consideration of this, we study three representative sparse signal recovery algorithms in landmark classification in this paper, namely, the basis pursuit algorithm (BP) [57], the SpaRSA approach [44], and the fast Laplace algorithm (FastLaplace) [58,59]. In BP algorithm, the ℓ_1 norm optimization in Eq. (2) is solved by reducing it to a linear problem and the primal-dual log-barrier algorithm is implemented for the signal estimation. The SpaRSA approach estimates the sparse signal by calculating the ℓ_2–ℓ_1 problem as

$$\min_{\boldsymbol{x} \in R^n} \frac{1}{2} \|\boldsymbol{y} - A\boldsymbol{x}\|_2^2 + \lambda \|\boldsymbol{x}\|_1 \tag{11}$$

where $\lambda > 0$ is the positive regularization coefficient and $\|\cdot\|_2$ denotes the Euclidean norm. In the fast Laplace algorithm, the Laplace prior is utilized to model the sparsity of the unknown

signal and the Bayesian framework is employed to formulate the sparse signal reconstruction problem in CS.

A detailed description of the proposed hybrid ELM-SRC landmark recognition framework is given in Algorithm 2.

Algorithm 2. The proposed ELM-SRC landmark recognition framework.

Given:

The SPK-BoW feature dictionary of training landmarks A;

The training landmark database $\mathcal{A} = \{(\mathbf{x}_i, \mathbf{t}_i)\}_{i=1}^{\mathbf{N}}$;

The number of landmark categories K;

The number of hidden neurons L and the threshold δ

Output:

(1) Randomly generated the hidden node parameters $\boldsymbol{a}_j \in \mathcal{R}^d$ and $b_j \in \mathcal{R}$ $(j = 1, 2, \ldots, L)$

(2) Training the ELM classifier using the landmark database $\mathcal{A}$

(3) For each testing landmark, extract its SPK-BoW histogram $\boldsymbol{y}$

(4) Calculate the neural network output $\boldsymbol{o}_y$ by ELM classifier of the testing landmark using $\boldsymbol{y}$

(5) Find the maximum entry o_p and the second largest entry o_s in $\boldsymbol{o}_y$

(6)
- **if** $o_p - o_s > \delta$
  - $c_y = \arg \min_{k \in [1,\ldots,K]} \{\boldsymbol{o}_y(k)\}$
- **else**
  - Estimate the sparse coefficient $\tilde{\boldsymbol{x}}$ through ℓ_1-minimization optimization
    - **for** $k = 1 : K$
    - Find the vector $\varphi_k(\tilde{\boldsymbol{x}})$
    - Calculate the residual $r(\tilde{\mathbf{y}}_k) = \|\boldsymbol{y} - \tilde{\mathbf{y}}_k\|_2$, with $\tilde{\mathbf{y}}_k = A\psi_k(\tilde{\boldsymbol{x}})$
    - $c_y = \arg \min_{k \in [1,\ldots,K]} \{r(\tilde{\mathbf{y}}_k)\}$
    - **end for**
- **end if**

4. Experiments

To evaluate the landmark recognition performance of the combination approach based on ELM and SRC (ELM-SRC), we test using the NTU campus landmark database [7,12] in our PC. The NTU's database contains 4156 images belonging to 50 different categories, including buildings, structures, and places of interests. For each patch of the landmark image, 200 features are extracted using the SPK-BoW approach and the recognition performance is compared under two schemes, i.e., using level 1 only (200 features) and using level 1 + level 2 together (1400 features). To show the efficiency of the SPK-BoW approach, the scalable vocabulary tree (SVT) landmark representation approach, which is involved to speed up the visual codebook generation and vector quantization process for SIFT features, is utilized for comparison. In the SVT approach, the vocabulary tree is generated by performing hierarchical **k**-means clustering algorithm iteratively on a set of local descriptors, until a predefined leaf nodes number is reached. First, an initial **k**-means algorithm is run on the training features to yield **k** cluster centers. The same process is then recursively applied to each new group to generate new centers. Each cluster

center and the **k**-means iteration number can be treated as the branch and depth of the tree, respectively. Fig. 6 shows the illustration of the SVT algorithm. In our comparisons, two different number of features are generated for landmark representation using the SVT approach, namely 225 and 1000, with the branch $=15$ and depth $=2$, and branch $=10$ and depth $=3$, respectively.

4.1. Comparison with ELM and SRC algorithm

The performance comparisons with ELM and SRC algorithm are given in this part. To show the efficiency of the combination approach, we list the average recognition rate and testing time per landmark image among multiple trials in Table 1 for comparisons. For each trial of experiment, the ratio of the training and testing landmarks is set to be 17:3. The experimental results of ELM, SRC and the hybrid algorithm ELM-SRC tested with the SPK-BoW feature extraction approach with 1400 features are provided. The three sparse estimators are adopted and the value of δ is set to be 0.2. As we can see, ELM enjoys the fastest recognition speed but has the lowest recognition rate. Using the same sparse signal recovery algorithm, the SRC algorithm achieves higher recognition accuracy than ELM-SRC. However, the recognition time per sample costed by the SRC algorithm is also several times longer than the one by ELM-SRC. In view of the fast response time and high classification rate requirements for landmark recognition application on mobile terminals, the ELM-SRC approach is more suitable to cater these requirements than ELM and SRC.

The choice of the δ affects the performance of the ELM-SRC algorithm. In general, the larger the value of δ is used, the higher the recognition rate of the ELM-SRC approach is. However, the

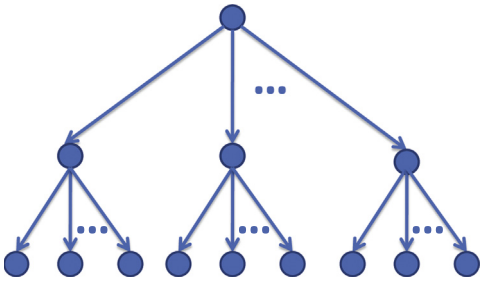

Fig. 6. Description of SVT.

Table 1
Comparisons on recognition rate and testing time per sample with $\delta=0.2$ and 1400 features.

Classifiers	Rate (%)	Time (s)
ELM	83.31	0.0164
SRC(SpaRSA)	93.11	24.3347
SRC(FastLaplace)	92.30	22.4429
SRC(BP)	90.69	15.9245
ELM-SRC(SpaRSA)	91.33	11.9787
ELM-SRC(FastLaplace)	90.72	8.5362
ELM-SRC(BP)	89.18	7.2676

average recognition time per sample also increases. This is because more query landmark samples are selected to process by the SRC approach in ELM-SRC. To verify these, we plot the average recognition rate and the average speedup of the recognition time per sample by the ELM-SRC algorithm w.r.t. three different values of $\delta = 0.05, \delta = 0.1, \delta = 0.2$ in Figs. 7 and 8, respectively. Here, for each sparse signal recovery algorithm used in the ELM-SRC, the speedup of the average recognition time per sample is computed against to the time spent by the same algorithm in the SRC approach. The curves shown in Figs. 7 and 8 demonstrate our statements. In addition, results listed in Table 1 and curves depicted in Fig. 7 reveal that the SpaRSA sparse signal estimator is more accurate in finding the associated representation samples for the NTU's campus landmark recognition.

The recognition performance of ELM, SRC and ELM-SRC algorithm w.r.t. different ratios of the training and testing landmarks is also studied in this section. We test four different percentages of the training data, namely, 60%, 70%, 80%, and 90%, respectively. For the ELM-

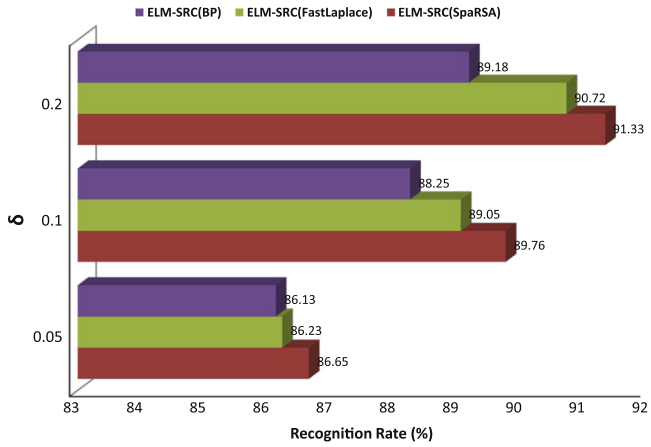

Fig. 7. Recognition rate by the ELM-SRC algorithm w.r.t. different δ values.

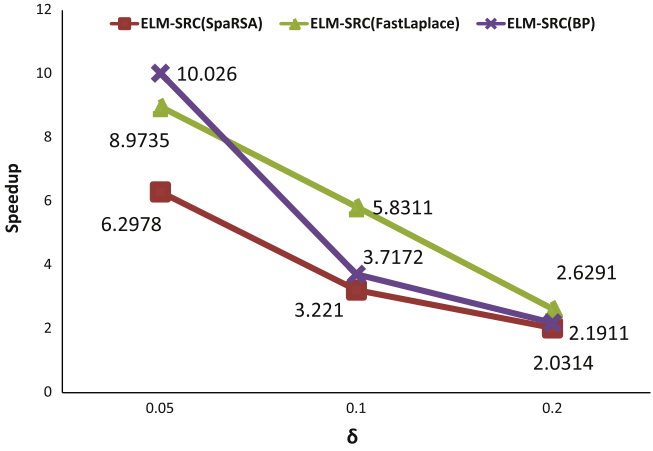

Fig. 8. Speedup by the ELM-SRC algorithm w.r.t. different δ values.

SRC approach, the performance with $\delta=0.2$ is compared. It is obvious that more samples have been used as the training data, higher classification rate can be achieved. For ELM, larger ratio of the training data means more information are available for classifier learning and construction. For SRC and ELM-SRC, as stated in [43], the critical factors for accurate recognition are correctly computing the sparse representation coefficients and sufficiently enough features for building the dictionary, which is indeed in line with the experimental results we have plotted in the figure (Fig. 9).

4.2. Comparison with the SVT approach

We compare the performance of the SPK-BoW landmark representation approach with the SVT feature extraction algorithm in this section. As the general trends of the recognition rate and the recognition time are similar for the three sparse signal recovery algorithms, we only show the comparisons with the SpaRSA estimator for the SRC approach and the ELM-SRC classifier in detail in this section. For all algorithms, the ratio of training and testing landmarks remains 17:3 and the threshold value δ is set to be 0.1. The average results including the recognition rate and the testing time are listed in Table 2 for illustration.

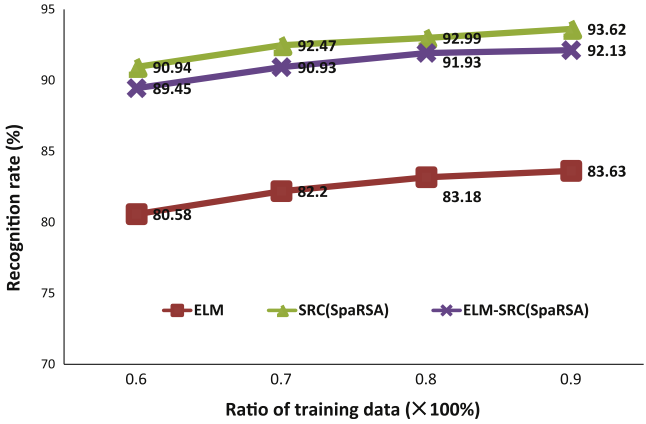

Fig. 9. Recognition rate comparison w.r.t. different ratios of the training and testing landmarks.

Table 2
Performance comparisons between SVT and SPK-BoW approaches.

Classifiers	Features							
	SVT				SPK-BoW			
	225		1000		200		1400	
	Rate (%)	Time (s)	Rate (%)	Time (s)	Rate (%)	Time (s)	Rate (%)	Time (s)
ELM	75.09	0.0112	76.47	0.0155	78.6	0.0087	83.31	0.0164
SRC(SpaRSA)	87.44	3.7214	89.73	19.2962	89	1.5878	93.11	24.3347
ELM-SRC(SpaRSA)	86.13	1.0211	87.45	7.7553	87.21	1.1981	91.33	11.9787

We can see from the table that for all three classifiers, adopting SPK-BoW features wins higher recognition rate than using SVT features when the number of features used by SPK-BoW is close to SVT, i.e., 200 in SPK-BoW vs 225 in SVT and 1400 in SPK-BoW vs 1000 in SVT. Using the same feature extraction method, the large number of features employed for classifier learning generally leads to better recognition performance than the one by small number of features. However, large number of features also suffer the long testing time issue. Likewise, the combination ELM-SRC approach is able to provide a higher recognition accuracy than ELM and a faster testing speed than SRC.

5. Conclusions

Landmark recognition with the sparse representation classification (SRC) has been studied recently. Comparing to conventional machine learning based approach, the SRC algorithm has the advantages of classifier training-free and high recognition rate properties. However, solving the sparse representation coefficients for query landmark brings an issue of long testing time to the SRC algorithm. To reduce the recognition time, we employed the feedforward artificial neural networks (FNN) trained with the popular ELM algorithm to speed up the testing process. The hybrid classifier which combines ELM and SRC for landmark recognition shown interesting results in both classification rate and recognition time. To exploit the spatial layout information of landmark images and emphasize the region of interests, we adopted the recent SPK-BoW approach for feature extraction and image representation. Detailed experimental results and comparisons conducted on the NTU campus landmark database have been provided for illustration. In the future work, we will investigate optimal algorithms which are more efficient to design the assessment scheme for the testing landmark image partition.

Acknowledgment

This work was supported by the Natural Science Foundation of Zhejiang Province, China, under Grant LY15F030017, the National Key Basic Research Program of China under Grant 2012CB821204, the National Natural Science Foundation of China under Grant 61175001, and the Key Program of National Natural Science Foundation of China under Grant 61333009.

References

[1] T. Chen, K. Wu, K.-H. Yap, Z. Li, F.S. Tsai, A survey on mobile landmark recognition for information retrieval, in: International Conference on Mobile Data Management: Systems, Services and Middleware, 2009, pp. 625–630.

[2] P. Bhattacharya, M. Gavrilova, A survey of landmark recognition using the Bag-of-Words framework, in: Intelligent Computer Graphics 2012, Studies in Computational Intelligence, vol. 441, 2013, pp. 243–263.

[3] Y.-T. Zheng, M. Zhao, Y. Song, H. Adam, U. Buddemeier, A. Bissacco, F. Brucher, T.-S. Chua, H. Neven, Tour the world: building a webscale landmark recognition engine, in: Proceedings of IEEE International Conference on Computer Vision and Pattern Recognition, 2009, pp. 1085–1092.

[4] A.R. Zamir, M. Shah, Accurate image localization based on Google Maps street view, in: Proceedings of European Conference on Computer Vision, vol. 6314, 2010, pp. 255–268.

[5] K.-H. Yap, T. Chen, Z. Li, K. Wu, A comparative study of mobilebased landmark recognition techniques, IEEE Intell. Syst. 25 (1) (2010) 48–57.

[6] T. Chen, K.-H. Yap, L.-P. Chau, Integrated content and context analysis for mobile landmark recognition, IEEE Trans. Circuits Syst. Video Technol. 21 (10) (2011) 1476–1486.

[7] T. Chen, K.-H. Yap, Discriminative BoW framework for mobile landmark recognition, IEEE Trans. Cybern. 44 (3) (2014) 695–706.
[8] J. Cao, T. Chen, J. Fan, Landmark recognition with compact BoW histogram and ensemble ELM, Multimedia Tools Appl. (2015), in press, http://dx.doi.org/10.1007/s11042-014-2424-1.
[9] A. Pinz, A. Fussenegger, M. Auer, Generic object recognition with boosting, IEEE Trans. Pattern Anal. Mach. Intell. 28 (2006) 416–431.
[10] F.-F. Li, P. Perona, A Bayesian hierarchical model for learning natural scene categories, in: Proceedings of IEEE Conference on Computer Vision and Pattern Recognition, 2005, pp. 524–531.
[11] B. Girod, V. Chandrasekhar, D.M. Chen, Mobile visual search, IEEE Signal Process. Mag. July (2011) 61–76.
[12] J. Cao, T. Chen, J. Fan, Fast online learning algorithm for landmark recognition based on BoW framework, in: Proceedings of 2014 IEEE Conference on Industrial Electronics and Applications, Hangzhou, China, June 9–11, 2014, pp. 1163–1168.
[13] C. Yin, S. Zhong, W. Chen, Design of sliding mode controller for a class of fractional-order chaotic systems, Commun. Nonlinear Sci. Numer. Simul. 17 (2012) 356–366.
[14] C. Yin, S. Dadras, S. Zhong, Y. Chen, Control of a novel class of fractional-order chaotic systems via adaptive sliding mode control approach, Appl. Math. Modell. 37 (4) (2013) 2469–2483.
[15] C. Yin, Y. Chen, S. Zhong, Fractional-order sliding mode based extremum seeking control of a class of nonlinear systems, Automatica 50 (2014) 3173–3181.
[16] Y. Li, J. Lim, Outdoor place recognition using compact local descriptors and multiple queries with user verification, in: Proceedings of 15th International Conference on Multimedia, Augsburg, Germany, September 2007, pp. 549–552.
[17] G. Fritz, C. Seifert, L. Paletta, A mobile vision system for urban detection with informative local descriptors, in: Proceedings of IEEE International Conference on Computer Vision and Systems, January 2006, pp. 30–35.
[18] S. Lazebnik, C. Schmid, J. Ponce, Beyond bags of features: spatial pyramid matching for recognizing natural scene categories, in: Proceedings of IEEE Conference on Computer Vision and Pattern Recognition, vol. 2, 2006, pp. 2169–2178.
[19] C. Cheng, D. Page, L. Abidi, Object-based place recognition and loop closing with jigsaw puzzle image segmentation algorithm, in: Proceedings of IEEE Conference on Robotics and Automation, Pasadena, CA, 2008, pp. 557–562.
[20] Y. Li, J. H. Lim, H. Goh, Cascaded classification with optimal candidate selection for effective place recognition, in: Proceedings of IEEE Conference on Multimedia, 2008, pp. 1493–1496.
[21] F. Scalzo, J.H. Piater, Adaptive patch features for object class recognition with learned hierarchical models, in: Proceedings of IEEE International Conference on Computer Vision and Pattern Recognition, 2007, pp. 1–8.
[22] G. Csurka, C. Dance, L. Fan, J. Willamowski, C. Bray, Visual categorization with bags of keypoints, in: Proceedings of International Workshop on Statistical Learning in Computer Vision, 2004.
[23] A. Bosch, A. Zisserman, X. Munoz, Scene classification using a hybrid generative/discriminative approach, IEEE Trans. Pattern Anal. Mach. Intell. 4 (April (3)) (2008) 712–726.
[24] R. Fergus, P. Perona, A. Zisserman, Object class recognition by unsupervised scale-invariant learning, in: Proceedings of IEEE International Conference Computer Vision and Pattern Recognition, vol. 2, 2003, pp. 264–271.
[25] T. Yeh, K. Tollmar, T. Darrell, Searching the web with mobile images for location recognition, in: Proceedings of IEEE Conference on Computer Vision and Pattern Recognition, 2004, pp. 76–81.
[26] Y. Ge, J. Yu, A scene recognition algorithm based on covariance descriptor, in: Proceedings of IEEE Conference on Cybernetics and Systems, 2008, pp. 838–842.
[27] O. Linde, T. Lindeberg, Object recognition using composed receptive field histograms of higher dimensionality, in: Proceedings of IEEE Conference on Image Processing and Pattern Recognition, 2004.
[28] A. Torralba, K.P. Murphy, W.T. Freeman, M.A. Rubin, Context-based vision system for place and object recognition, in: Proceedings of IEEE International Conference on Computer Vision, 2003, pp. 273–280.
[29] L. Lu, K. Toyama, G.D. Hagar, A two level approach for scene recognition, in: Proceedings of IEEE International Conference on Computer Vision and Pattern Recognition, vol. 1, 2005, pp. 688–695.
[30] D. Parikh, C.L. Zitnick, T. Chen, Determining patch saliency using low-level context, in: Proceedings of 10th European Conference on Computer Vision, 2008, pp. 446–459.
[31] J. Lim, Y. Li, Y. You, Scene recognition with camera phones for tourist information access, in: Proceedings of International Conference on Multimedia, 2007, pp. 100–103.
[32] D. Lowe, Distinctive image features from scale-invariant keypoints, Int. J. Comput. Vis. 60 (2004) 91–110.
[33] J. Sivic, A. Zisserman, Video Google: a text retrieval approach to object matching in videos, in: Proceedings of IEEE International Conference on Computer Vision, 2003, pp. 1470–1478.

[34] S. Pronobis, A. Caputo, Confidence-based cue integration for visual place recognition, in: Proceedings of IEEE Conference on Intelligent Robots and Systems, San Diego, CA, 2007, pp. 2394–2401.
[35] D. Nister, H. Stewenius, Scalable recognition with a vocabulary tree, in: Proceedings of IEEE International Conference on Computer Vision and Pattern Recognition, vol. 2, 2006, pp. 2161–2168.
[36] G.-B. Huang, Q.-Y. Zhu, C.-K. Siew, Extreme learning machine: theory and applications, Neurocomputing 70 (2006) 489–501.
[37] J. Cao, Z. Lin, G.-B. Huang, Composite function wavelet neural networks with extreme learning machine, Neurocomputing 73 (2010) 1405–1416.
[38] G.-B. Huang, H. Zhou, X. Ding, R. Zhang, Extreme learning machine for regression and multiclass classification, IEEE Trans. Syst. Man Cybern. – Part B: Cybernetics 42 (2012) 513–529.
[39] N. Liu, H. Wang, Ensemble based extreme learning machine, IEEE Signal Process. Lett. 17 (8) (2010) 754–757.
[40] J. Cao, Z. Lin, G.-B. Huang, N. Liu, Voting based extreme learning machine, Inf. Sci. 185 (2012) 66–77.
[41] J. Cao, Z. Lin, G.-B. Huang, Voting base online sequential extreme learning machine for multi-class classification, in: Proceedings of IEEE International Symposium on Circuits and Systems, 2013, pp. 2327–2330.
[42] J. Cao, L. Xiong, Protein sequence classification with improved extreme learning machine algorithms, BioMed Res. Int. 2014 (2014) 12 pp., Article ID 103054, http://dx.doi.org/10.1155/2014/103054.
[43] J. Wright, A.Y. Yang, A. Ganesh, S. Sastry, Y. Ma, Robust face recognition via sparse representation, IEEE Trans. Pattern Anal. Mach. Intell. 31 (2) (2009) 210–226.
[44] S. Wright, R. Nowak, M. Figueiredo, Sparse reconstruction by separable approximate, IEEE Trans. Signal Process. 57 (7) (2009) 2479–2493.
[45] B. Olshausen, D. Field, Emergency of simple-cell receptive field properties by learning a sparse coding for natural images, Nature 381 (6583) (1996) 607–609.
[46] W. Vinje, J. Gallant, Sparse coding and decorrelation in primary visual cortex during natural vision, Science 287 (5456) (2000) 1273–1276.
[47] M. Luo, F. Sun, H. Liu, Joint block structure sparse representation for multi-input–multi-output (MIMO) T–S fuzzy system identification, IEEE Trans. Fuzzy Syst. 22 (6) (2014) 1387–1400.
[48] D. Donoho, Compressed sensing, IEEE Trans. Inf. Theory 52 (4) (2006) 1289–1306.
[49] E. Cand e' s, Compressive sampling, in: Proceedings of International Congress of Mathematicians, 2006.
[50] J. Cao, Z. Lin, The detection bound of the probability of error in compressed sensing using Bayesian approach, in: Proceedings of IEEE International Symposium on Circuits and Systems, 2012, pp. 2577–2580.
[51] J. Cao, Z. Lin, Bayesian signal detection with compressed measurements, Inf. Sci. 289 (2014) 241–253.
[52] J. Tropp, A. Gilbert, Signal recovery from random measurements via orthogonal matching pursuit, IEEE Trans. Inf. Theory 53 (12) (2006) 5406–5425.
[53] J. Cao, Y. Zhao, X. Lai, T. Chen, B. Mirza, Z. Lin, Landmark recognition via sparse representation, in: IEEE International Conference on Digital Signal Processing, Singapore, 2015, accepted for publication.
[54] M. Luo, K. Zhang, A hybrid approach combining extreme learning machine and sparse representation for image classification, Eng. Appl. Artif. Intel. 27 (2014) 228–235.
[55] G.-B. Huang, L. Chen, C.-K. Siew, Universal approximation using incremental constructive feedforward networks with random hidden nodes, IEEE Trans. Neural Netw. 17 (4) (2006) 879–892.
[56] G.-B. Huang, An insight into extreme learning machines: random neurons, random features and kernels, Cogn. Comput. 6 (3) (2014) 376–390.
[57] S. Chen, D. Donoho, M. Saunders, Atomic decomposition by basis pursuit, SIAM J. Sci. Comput. 20 (1) (1998) 33–61.
[58] S. Ji, Y. Xue, L. Carin, Bayesian compressive sensing, IEEE Trans. Image Process. 56 (6) (2008) 2346–2356.
[59] S. Babacan, R. Molina, A. Katsaggelos, Bayesian compressive sensing using Laplace priors, IEEE Trans. Image Process. 19 (1) (2010) 53–63.